

# Continuous monitoring measured signals bounded by past and future conditions in enlarged quantum systems

Le Bin Ho<sup>1,2,\*</sup>

<sup>1</sup>*Department of Physics, Kindai University, Higashi-Osaka, 577-8502, Japan,*

<sup>2</sup>*Ho Chi Minh City Institute of Physics, VAST, Ho Chi Minh City, Viet Nam*

In a quantum system that is bounded by past and future conditions, weak continuous monitoring forward-evolving and backward-evolving quantum states are usually carried out separately. Therefore, measured signals at a given time  $t$  cannot be monitored continuously. Here, we propose an *enlarged-quantum-system* method to combine these two processes together. Therein, we introduce an enlarged quantum state that contains both the forward- and backward-evolving quantum states. The enlarged state is governed by an enlarged master equation and propagates one-way forward in time. As a result, the measured signals at time  $t$  can be monitored continuously and can provide advantages in the signals amplification and signal processing techniques. Our proposal can be implemented on various physical systems, such as superconducting circuits, NMR systems, ion-traps, quantum photonics, and among others.

PACS numbers: 03.65.Aa, 03.65.Ca, 03.65.Ta

## I. INTRODUCTION

In quantum mechanics, measurement results at a given time can be predicted from the system of interest that propagates forward in time from past conditions. Instead, if the system is bounded by future conditions and propagates backward in time, then the results are exactly the time reversal of the former case when the past and the future conditions are prepared in the same state [1–3]. This is the time-reversal symmetry in quantum mechanics (see Ref. [4] for reconstructing the time-reversal symmetry.) Nonetheless, weak measurements that are bounded by both the past and the future conditions can affect the statistical results and provide more information about the measured system [5, 6]. In this case, a time-dependent weak value can be defined by incorporating both a *forward-evolving state* and a *backward-evolving state* at the same given time [7, 8]. However, it neither be obtained directly nor be monitored continuously because the quantum trajectories of the forward- and backward-evolving states are obtained separately [1–4, 9–11]. It implies that the measured system does not evolve causally from the past to the future. This is a *noncausal* problem in the measurements based on the two-state-vector formalism [12]. Monitoring a system continuously over time can help to characterize the stochastic dynamics of the system during the measurement and also might useful for quantum state reconstruction and parameter estimation theory [13]. Therefore, it is also beneficial and demand to monitor time-dependent weak values continuously.

In this paper, to solve the noncausal problem and obtain the continuous monitoring, we propose an *enlarged-quantum-system* method, therein we map both the forward- and the backward-evolving states onto an enlarged quantum state. The enlarged quantum state can

propagate casually one-way forward in time that is governed by an enlarged master equation. We also introduce a *two-time correlation weak value*, where we show that it can be monitored continuously in the enlarged system. We illustrate our proposal in a superconducting qubit driven at resonance based on the experiments in Refs. [1–3]. Afterward, we also discuss how to implement the enlarged system in various physical platforms, such as superconducting circuits, NMR systems, ion-traps, and quantum photonics systems.

The structure of this paper is organized as follows. Section II introduces an enlarged system where both the forward- and backward-evolving states are embedded onto an enlarged state. The master equation that governs the evolution of the enlarged state is also discussed. We introduce the two-time correlation weak value in Sec. III and illustrate it in Sec. IV. In Sec. V, we discuss the implementation of the enlarged system. The paper concludes with a discussion and a brief summary in Sec. VI.

## II. ENLARGED QUANTUM SYSTEM

### A. Enlarged quantum state

We first describe a mapping process that maps two arbitrary states, such as  $\rho$  and  $E$  in an original system ( $\mathcal{OS}$ ) onto an enlarged state  $\varrho$  in an enlarged system ( $\mathcal{ES}$ ). In the  $\mathcal{OS}$ , the complex Hilbert space of a  $d$ -dimensional vector is denoted as  $\mathbb{C}_d$  and the complex Hilbert space of a  $d \times d$  density matrix is set to be  $L(\mathbb{C}_d)$ . We consider a mapping process from the original Hilbert space  $L(\mathbb{C}_d)$  to an enlarged Hilbert space  $L(\mathbb{C}_2 \otimes \mathbb{C}_d)$  that maps both  $\rho$  and  $E$  onto  $\varrho$  in the following

$$\varrho_t = \frac{1}{2} \begin{pmatrix} \rho_\tau & 0_d \\ 0_d & E_{\tau'} \end{pmatrix}, \quad (1)$$

---

\* Electronic address: binho@kindai.ac.jp

where  $0_d \in L(\mathbb{C}_d)$  is a  $d \times d$  zero matrix. Factor  $\frac{1}{2}$  is used for the normalization. In the following subsection, we will choose  $\rho$  as a forward-evolving state and  $E$  as a backward-evolving state. For now, however, we treat them in general forms. We note that  $t$ ,  $\tau$ , and  $\tau'$  are different, in general. A similar mapping process for pure quantum states has been introduced previously [12]. This mapping can be implemented by adding an ancillary qubit to the  $\mathcal{OS}$  such that  $\varrho_t = [|0\rangle\langle 0| \otimes \rho_\tau + |1\rangle\langle 1| \otimes E_{\tau'}]/2$ , where  $|0\rangle \equiv \begin{pmatrix} 1 \\ 0 \end{pmatrix}$  and  $|1\rangle \equiv \begin{pmatrix} 0 \\ 1 \end{pmatrix}$  are the bases of the ancillary qubit. Recently, similar mapping has been extensively studied both in theoretical and experimental [14–23]. The states in the  $\mathcal{OS}$  can be decoded by the inversions

$$\rho_\tau = 2\mathcal{M}\varrho_t\mathcal{N} \text{ and } E_{\tau'} = 2\mathcal{M}\varrho_t(\sigma_x \otimes \mathbf{I}_n)\mathcal{N}, \quad (2)$$

where  $\mathcal{M} = (1, 1) \otimes \mathbf{I}_d$  and  $\mathcal{N} = \begin{pmatrix} 1 \\ 0 \end{pmatrix} \otimes \mathbf{I}_d$ , where  $\mathbf{I}_d \in L(\mathbb{C}_d)$  is a  $d \times d$  identity matrix.

### B. Enlarged master equation

Now we describe the master equation in the  $\mathcal{ES}$ . We consider the case that the  $\mathcal{OS}$  is bounded by a past condition  $\rho_0$  and a future condition  $E_T$  for a time interval  $[0, T]$ . The forward-evolving state  $\rho_t$  satisfies the Lindblad master equation [24, 25]

$$\frac{d\rho_t}{dt} = -\frac{i}{\hbar}[\mathbf{H}, \rho_t] + \sum_n \frac{1}{2} \left[ 2\mathbf{C}_n \rho_t \mathbf{C}_n^\dagger - \{\mathbf{C}_n^\dagger \mathbf{C}_n, \rho_t\} \right], \quad (3)$$

which propagates forward in time from  $t = 0$  to  $t$ , where  $\mathbf{H} \in L(\mathbb{C}_d)$  is the Hamiltonian of the  $\mathcal{OS}$ ,  $\mathbf{C}_n = \sqrt{k_n} \mathbf{A}_n$  is a Lindblad operator  $\in L(\mathbb{C}_d)$ , that describes the effect of the environment in the Markov approximation, and  $\mathbf{A}_n$  is an operator through which the environment couples to the system with a relaxation rate  $k_n$ . Similarly, the Lindblad master equation, which governs the evolution of the backward-evolving state  $E$ , is given by [1–3, 26]

$$\frac{dE_t}{dt} = -\frac{i}{\hbar}[\mathbf{H}, E_t] - \sum_n \frac{1}{2} \left[ 2\mathbf{C}_n^\dagger E_t \mathbf{C}_n - \{\mathbf{C}_n^\dagger \mathbf{C}_n, E_t\} \right], \quad (4)$$

which propagates backward in time from  $T$  to  $t \leq T$ . We note that in the time interval  $t \in [0, T]$ , this backward evolution has a *forward version* that evolves forward in time and satisfies the time-reversal-symmetry property [4]. More precisely, the quantum trajectory of the backward evolution,  $E_t$ , has a time-reversal trajectory,  $E_{T-t}$ . (See Appendix A). The forward version is

$$\begin{aligned} \frac{dE_{T-t}}{dt} &= \frac{i}{\hbar}[\mathbf{H}, E_{T-t}] \\ &+ \sum_n \frac{1}{2} \left[ 2\mathbf{C}_n^\dagger E_{T-t} \mathbf{C}_n - \{\mathbf{C}_n^\dagger \mathbf{C}_n, E_{T-t}\} \right], \end{aligned} \quad (5)$$

where its solution at time  $t$  is  $E_{T-t}$ .

Notable that Eqs. (3, 5) evolve forward in time. We, therefore, combine them into an enlarged master equation which governs the enlarged state one-way forward in time as follows

$$\frac{d\varrho_t}{dt} = -\frac{i}{\hbar}[\mathcal{H}, \varrho_t] + \sum_n \frac{1}{2} \left[ 2\mathbf{C}_n \varrho_t \mathbf{C}_n^\dagger - \{\bar{\mathbf{C}}_n^\dagger \bar{\mathbf{C}}_n, \varrho_t\} \right], \quad (6)$$

where we have defined the enlarged Hamiltonian  $\mathcal{H} \equiv \sigma_z \otimes \mathbf{H}$ , the Lindblad operator  $\mathbf{C} \equiv |0\rangle\langle 0| \otimes \mathbf{C} + |1\rangle\langle 1| \otimes \mathbf{C}^\dagger$ , and  $\bar{\mathbf{C}} \equiv \mathbf{I}_2 \otimes \mathbf{C}$  in the  $L(\mathbb{C}_2 \otimes \mathbb{C}_d)$  enlarged Hilbert space. The solution  $\varrho_t$  at time  $t$  is given by  $\varrho_t$  in Eq. (1) where

$$\varrho_t = \frac{1}{2} \begin{pmatrix} \rho_t & 0_d \\ 0_d & E_{T-t} \end{pmatrix}. \quad (7)$$

The enlarged trajectory (described by  $\varrho_t$ ) can be measured continuously by monitoring the  $\mathcal{ES}$  forwardly in time.

We emphasize that the enlarged state  $\varrho_t$  is different from the “two-state” or “density state” defined by Reznik and Aharonov [27] and later used by [28–30]. In their original proposal, the density state is formed by putting the pre- and postselected states in such a way that  $\wp_t \equiv |\psi_t\rangle\langle \phi_t|$ , where  $\wp_t$  is the density state,  $|\psi_t\rangle$  and  $|\phi_t\rangle$  are pre- and postselected states, respectively. Recently, Vaidman et al. [31] also defined a so-called “genuine mixed two-state vector” where  $\wp_t \equiv (E_t, \rho_t)$ . Even in this case, the mapping is also different from ours: While Vaidman’s mapping is  $L(\mathbb{C}_d) \rightarrow \mathbb{C}_2 \otimes L(\mathbb{C}_d)$ , our mapping is  $L(\mathbb{C}_d) \rightarrow L(\mathbb{C}_2 \otimes \mathbb{C}_d)$ . Moreover, as we can see from Eq. (7),  $\rho_t$  and  $E_{T-t}$  are different in time, while previous studies require a consistent time.

## III. TWO-TIME CORRELATION WEAK VALUE

### A. Conventional time-dependent weak value

In a conventional weak measurement, the conventional time-dependent weak value is described by both the forward-evolving state  $\rho_t$  immediately before the weak measurement was carried out and the backward-evolving state  $E_t$  immediately after the measurement [5, 32]. The conventional time-dependent weak value for an observable  $\mathbf{A}$  at time  $t$  is given by [7, 8, 31]

$$\langle \mathbf{A}_t \rangle_w = \frac{\text{Tr}[E_t \mathbf{A} \rho_t]}{\text{Tr}[E_t \rho_t]}, \quad (8)$$

where the subscript w stands for “weak value.”

We now describe the conventional time-dependent weak value in the  $\mathcal{ES}$ . From Eq. (2) we have

$$\rho_t = 2\mathcal{M}\varrho_t\mathcal{N} \text{ and } E_{\tau'} = 2\mathcal{M}\varrho_t(\sigma_x \otimes \mathbf{I}_n)\mathcal{N}. \quad (9)$$

Using the time-reversal evolution, we can derive  $E_t = 2\mathcal{M}\varrho_{T-t}(\sigma_x \otimes \mathbf{I}_n)\mathcal{N}$ . Substituting  $\rho_t$  and  $E_t$  to Eq. (8)

we obtain

$$\langle \mathbf{A}_t \rangle_w = \frac{\text{Tr}[\mathcal{M}_{\varrho_{T-t}}(\sigma_x \otimes \mathbf{I}_d) \mathcal{N} \mathbf{A} \mathcal{M}_{\varrho_t} \mathcal{N}]}{\text{Tr}[\mathcal{M}_{\varrho_{T-t}}(\sigma_x \otimes \mathbf{I}_d) \mathcal{N} \mathcal{M}_{\varrho_t} \mathcal{N}]}.$$
 (10)

Clearly,  $\langle \mathbf{A}_t \rangle_w$  depends on both  $\varrho_t$  and  $\varrho_{T-t}$ . Therefore, it cannot be measured continuously in time even for the  $\mathcal{ES}$  case.

### B. Two-time correlation weak value

To enjoy the benefit of the  $\mathcal{ES}$ , we introduce a so-called *two-time correlation* weak value in a very similar way that

$$\langle \mathbf{A}_{t,T-t} \rangle_w^c = \frac{\text{Tr}[E_{T-t} \mathbf{A} \rho_t]}{\text{Tr}[E_{T-t} \rho_t]},$$
 (11)

where the superscript *c* represents “two-time correlation.” Following are some properties of the two-time correlation weak value.

(i) It is different from the conventional weak value: while the conventional weak value is conditioned on  $\rho_t$  and  $E_t$ , the two-time correlation weak value is described by  $\rho_t$  and  $E_{T-t}$ , as we depict in Fig. 1. Obviously, it depends on two different times, which are correlated, i.e.,  $t$  and  $T-t$ . It coincides with the conventional weak value only at  $t = T/2$ , i.e.,  $t = T-t$ .

(ii) The two-time correlation weak value defined by Eq. (11) is a mathematical concept and thus, cannot be realized in the  $\mathcal{OS}$ .

(iii) However, in the  $\mathcal{ES}$ , we point out that the two-time correlation weak value is an expectation value which can be measured continuously in time. Substituting Eq. (9) to Eq. (11) we obtain

$$\langle \mathbf{A}_{t,T-t} \rangle_w^c = \frac{\text{Tr}[\mathcal{M}_{\varrho_t}(\sigma_x \otimes \mathbf{I}_d) \mathcal{N} \mathbf{A} \mathcal{M}_{\varrho_t} \mathcal{N}]}{\text{Tr}[\mathcal{M}_{\varrho_t}(\sigma_x \otimes \mathbf{I}_d) \mathcal{N} \mathcal{M}_{\varrho_t} \mathcal{N}]} = \frac{\text{Tr}[\mathbf{A} \tilde{\varrho}_t]}{\text{Tr}[\tilde{\varrho}_t]},$$
 (12)

where  $\tilde{\varrho}_t \equiv \mathcal{M}_{\varrho_t} \mathcal{N} \mathcal{M}_{\varrho_t}(\sigma_x \otimes \mathbf{I}_d) \mathcal{N}$ . In this form, the two-time correlation weak value depends only on  $\varrho_t$  at time  $t$ . Therefore, it can be monitored continuously at each time  $t$  from 0 to  $T$  causally. In comparison to Eq. (10), the two-time correlation weak value Eq. (12) is more promising for continuous monitoring signals.

(iv) Furthermore, two-time correlation weak values are also useful for signals amplification and signals processing. It can be seen that the two-time correlation weak value can exceed outside the normal range of the observable eigenvalues with a proper choice of the pre- and post-selected density states  $\rho_0$  and  $E_T$ . See our illustration in Figs. 3, 4 below for the continuous monitoring signals, signals amplification, and signals processing.

It is also worthwhile to note that Aharonov et al. have discussed the concept of multiple-time states and multiple-time measurements [33]. However, we note that it is different from our “two-time correlation” here. In their work, they consider multiple preparations and

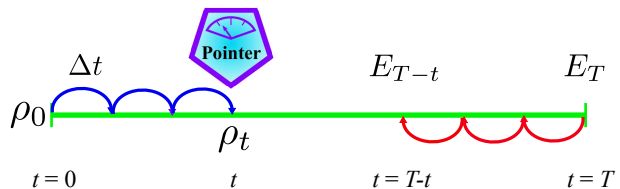


FIG. 1. (Color online) Graphical scheme for two-time correlation weak values. A quantum system is prepared in  $\rho_0$  and post-selected onto  $E_T$ . The initial state propagates forward in time to  $t$ , which we name as the forward-evolving state  $\rho_t$ . The final state propagates backward from  $T$  to  $T-t$ , which we denote as the backward-evolving state  $E_{T-t}$ . We also assume there are no further measurements after time  $T$ . For continuous measurements, the pointer is shifted (in time scale) after each time interval  $\Delta t$ . We emphasize that this measurement scheme is different from the original motivation by Aharonov et al., who consider a conventional weak value at time  $t$  described by  $\rho_t$  and  $E_t$  [5]. Even though this scheme cannot realize in an  $\mathcal{OS}$ , its two-time correlation weak value can be obtained continuously in an  $\mathcal{ES}$  as we show in the main text.

measurements, such that *preparation*  $\rightarrow$  *measurement*  $\rightarrow$  *preparation*  $\rightarrow$  *measurement*  $\rightarrow$  ... For a “two-time state,” in their words, it means *preparation*  $\rightarrow$  *measurement*  $\rightarrow$  *preparation*, or in other words, it implies *preparation*  $\rightarrow$  *measurement*  $\rightarrow$  *postselection*. In our work here, we consider only this situation and require no further measurements after the postselection. Their “two-time state” means time in the preparation and time in the postselection. Whereas, by “two-time correlation” in this work, it means two times in between the preparation time and postselection time. Furthermore, in our work, we consider such two-time correlation weak values in an  $\mathcal{ES}$  while the previous study did not.

## IV. ILLUSTRATION

To illustrate our proposal for some physical problems, we first consider an example based on a superconducting qubit driven at resonance as experimentally studied in Ref. [1], where the qubit is coupled to a waveguide cavity [34–37]. So far, weak measurements under the presence of decoherence have been investigated but they focused only on the  $\mathcal{OS}$ , where the continuous monitoring is not discussed [28, 38]. Here, we consider such problem in the  $\mathcal{ES}$  with our two-time correlation weak values. We will analyze the conventional weak value and two-time correlation weak value of the fluorescence signal, the atom population, and the photon number in some concrete models. We show that in the case of two-time correlation weak value, these measured signals can be detected continuously in the  $\mathcal{ES}$ .

A specific model of a two-level atom, which is driven by a laser field at the Rabi oscillations, oscillates between the ground state  $|g\rangle$  and the excited state  $|e\rangle$ . These oscillations emit a so-called fluorescence signal, which is

detected due to the transition from the excited state to the ground state. Its amplitude is proportional to the average value of the lowering operator  $\langle \sigma_- \rangle$  [1]. In the rotating wave approximation, we write the laser Hamiltonian as  $\mathbf{H}_L = \hbar\Omega\sigma_y/2$ , where  $\Omega$  is the Rabi frequency. The Lindblad operator is  $\mathbf{C} = \sqrt{k}\sigma_-$ . In this model, the forward master equation which governs the forward-evolving state  $\rho$  is given by

$$\frac{d\rho_t}{dt} = -\frac{i\Omega}{2}[\sigma_y, \rho_t] + k[\sigma_- \rho_t \sigma_+ - \frac{1}{2}\{\sigma_+ \sigma_-, \rho_t\}]. \quad (13)$$

The backward-evolving state  $E$  is governed backward in time by a corresponding adjoint equation as

$$\frac{dE_t}{dt} = -\frac{i\Omega}{2}[\sigma_y, E_t] - k[\sigma_+ E_t \sigma_- - \frac{1}{2}\{\sigma_+ \sigma_-, E_t\}], \quad (14)$$

where we have used the standard Pauli matrices  $\sigma_z = |e\rangle\langle e| - |g\rangle\langle g|$  and  $\sigma_y = i(\sigma_- - \sigma_+)$ . The enlarged master equation Eq. (6) takes the form

$$\frac{d\varrho_t}{dt} = -\frac{i\Omega}{2}[\sigma_z \otimes \sigma_y, \varrho_t] + k[\mathbf{C}\varrho_t\mathbf{C}^\dagger - \frac{1}{2}\{\bar{\mathbf{C}}^\dagger\bar{\mathbf{C}}, \varrho_t\}], \quad (15)$$

where  $\mathbf{C} = |0\rangle\langle 0| \otimes \sigma_- + |1\rangle\langle 1| \otimes \sigma_+$  and  $\bar{\mathbf{C}} = \mathbf{I}_2 \otimes \sigma_-$ . Solving this enlarged equation will give the enlarged state  $\varrho_t$  at any time  $t \in [0, T]$ .

For concreteness, we choose the parameters as  $\Omega/2\pi = 1.16$  MHz,  $k/2\pi = 95$  kHz [2]. The past condition at time  $t = 0$  is  $\rho_0 = |g\rangle\langle g|$  and the future condition at time  $T$  is  $E_T = |g\rangle\langle g|$ . We next examine the measured signals: the atom population  $\langle \sigma_z \rangle$ , the photon number  $\langle n \rangle$ , and the fluorescence signal  $\langle \sigma_- \rangle$ .

A measured signal can be detected by continuously monitoring the cavity, which can be described by the theory of POVM. For example, the measurement of the voltage signal  $V$ , that describes the atom population  $\langle \sigma_z \rangle$ , is given by the POVM operator as [2, 3]

$$\Omega_V = (2\pi a^2)^{-1/4} e^{-(V - \sigma_z)^2/4a^2}. \quad (16)$$

The probability of the outcome  $V$  that depends only on the enlarged state is shown in Appendix B, where

$$\begin{aligned} P(V) &= \frac{\text{Tr}(\Omega_V \rho_t \Omega_V^\dagger E_t)}{\sum_V \text{Tr}(\Omega_V \rho_t \Omega_V^\dagger E_t)} \\ &\propto \varrho_t^{00} \varrho_{T-t}^{22} e^{-(V-1)^2/2a^2} + \varrho_t^{11} \varrho_{T-t}^{33} e^{-(V+1)^2/2a^2} \\ &\quad + (\varrho_t^{10} \varrho_{T-t}^{23} + \varrho_t^{01} \varrho_{T-t}^{32}) e^{-(V^2+1)/2a^2}, \end{aligned} \quad (17)$$

where  $\varrho^{ij}$  are the elements of the enlarged density matrix. The conventional weak value of the voltage signal is given by  $\langle V \rangle_w = \int P(V) V dV$ , and can be evaluated

$$\langle V \rangle_w = \frac{\varrho_t^{00} \varrho_{T-t}^{22} - \varrho_t^{11} \varrho_{T-t}^{33}}{\varrho_t^{00} \varrho_{T-t}^{22} + \varrho_t^{11} \varrho_{T-t}^{33} + \varrho_t^{10} \varrho_{T-t}^{23} + \varrho_t^{01} \varrho_{T-t}^{32}}. \quad (18)$$

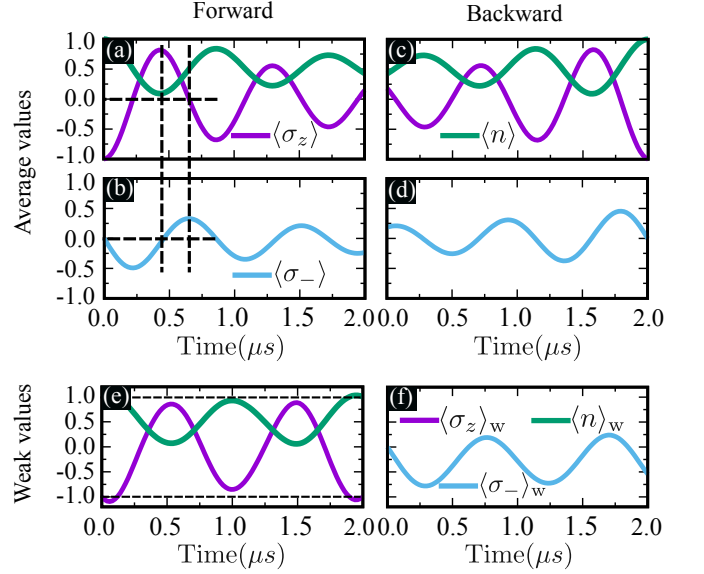


FIG. 2. (Color online) The average values and conventional weak values of the measured signals: the atom population  $\langle \sigma_z \rangle$  (dark-violet curves), the photon number  $\langle n \rangle$  (vine-green curves), and the fluorescence signal  $\langle \sigma_- \rangle$  (soft-blue) in a two-level atom. (a, b): The measured values correspond to the system that prepared in the density state  $\rho_0 = |g\rangle\langle g|$  at time  $t = 0$ . The forward-evolving state at time  $t$  is given by Eq. (13) and propagates forward in time. (c) and (d) show the same measured values correspond to the system that post-selected onto the density state  $E_T = |g\rangle\langle g|$  at time  $T$ . The backward-evolving state at time  $t$  is given by Eq. (14) and propagates backward in time. (e) and (f) represent the conventional weak values of the atom population  $\langle \sigma_z \rangle_w$ , the photon number  $\langle n \rangle_w$ , and the fluorescence signal  $\langle \sigma_- \rangle_w$  correspond to the system prepared in the state  $\rho_0$  at time  $t = 0$  and postselected onto the state  $E_T$  at time  $T$ . These conventional weak values can be obtained by both methods as shown in Eqs. (8, 10), where the enlarged quantum state at time  $t$  is given by Eq. (15) and propagates forward in time.

For the two-time correlation weak value, it yields

$$\langle V \rangle_w^c = \frac{\varrho_t^{00} \varrho_t^{22} - \varrho_t^{11} \varrho_t^{33}}{\varrho_t^{00} \varrho_t^{22} + \varrho_t^{11} \varrho_t^{33} + \varrho_t^{10} \varrho_t^{23} + \varrho_t^{01} \varrho_t^{32}}. \quad (19)$$

Note that in this section we omit  $t$  and  $T - t$  in the conventional weak value and two-time weak value.

Fig. 2(a) shows the average expectation values of the atom population and the photon number conditioned on the forward-evolving state, e.g.,  $\langle \sigma_z \rangle = \text{Tr}[\rho_t \sigma_z]$ . The results show the gradual dephasing of the atom due to the interaction [1, 2]. The atom population is bounded in the interval  $[-1, +1]$ . It is a  $\pi$ -phase difference from the photon number which implies that the atom absorbs photons to transfer from the ground state  $|g\rangle$  to the excited state  $|e\rangle$  and vice versa. In Fig. 2(b), the fluorescence signal, which is also conditioned on the forward-evolving state, is the  $\pi/2$ -phase difference from the atom population. In detail, starting from the maximum atom population (excited state), the fluorescence signal is zero. Then,

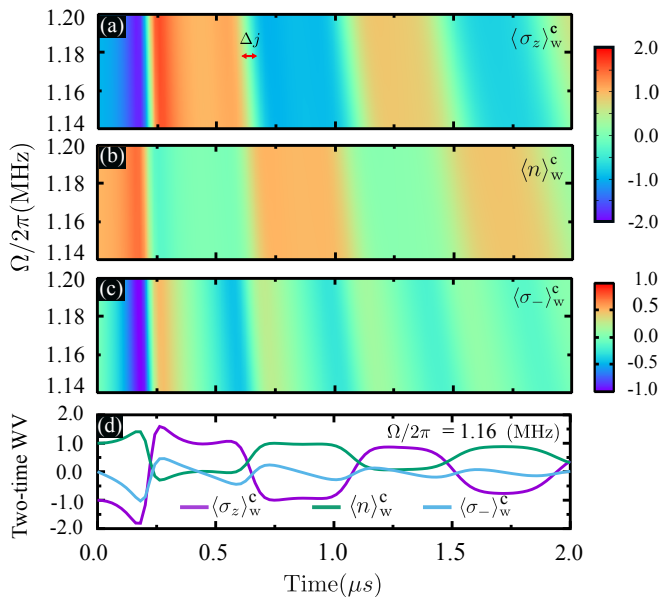


FIG. 3. (Color online) Two-time correlation weak values of the atom population  $\langle \sigma_z \rangle_w^c$  (a), the photon number  $\langle n \rangle_w^c$  (b), and the fluorescence signal  $\langle \sigma_- \rangle_w^c$  (c) in a wide range of frequency  $\Omega$ . (d) Extracted results at  $\Omega/2\pi = 1.16$  MHz.

during the relaxation from the maximum to zero of the atom population, the fluorescence signal increases and reaches the maximum as shown by the dash lines in Fig. 2(a, b). The process keeps going afterward. Similarly, Fig. 2(c, d) examine the average values of the measured signals conditioned on the backward-evolving state, e.g.,  $\langle \sigma_z \rangle = \text{Tr}[E_t \sigma_z]$ . In this case, the atom population and the photon number are damped backward in time and equal to the time reversal of the measured signals in Fig. 2(a) while the fluorescence signal reverts both the time and sign in comparison to the former case Fig. 2(b). The conventional weak values of these measured signals conditioned on both the forward- and backward-evolving states are shown in Fig. 2(e, f). Notable, the results do not “damp” and can exceed beyond their normal intervals due to the interference between the forward- and backward-evolving states [1].

We next consider the two-time correlation weak values of these measured signals. Figure 3(a-c) show the two-time correlation weak values of the atom population  $\langle \sigma_z \rangle_w^c$  (a), the photon number  $\langle n \rangle_w^c$  (b), and the fluorescence signal  $\langle \sigma_- \rangle_w^c$  (c) in a wide range of the frequency  $\Omega$ . Interestingly, these results do not behave Rabi oscillations. Indeed, the atom population exhibits a “quantum jump” in between the ground state (blue areas) and the excited state (red areas). We define a “jump-duration” ( $\Delta j$ ) which is a necessary time interval for the atom state jumps from one state to another. This jump-duration increases in time for each fixed frequency. Along with this atom jumps, the photon number can be detected (red areas) or not (green areas,) respectively (Fig.3(b).) Besides the jumping durations, the atom population and

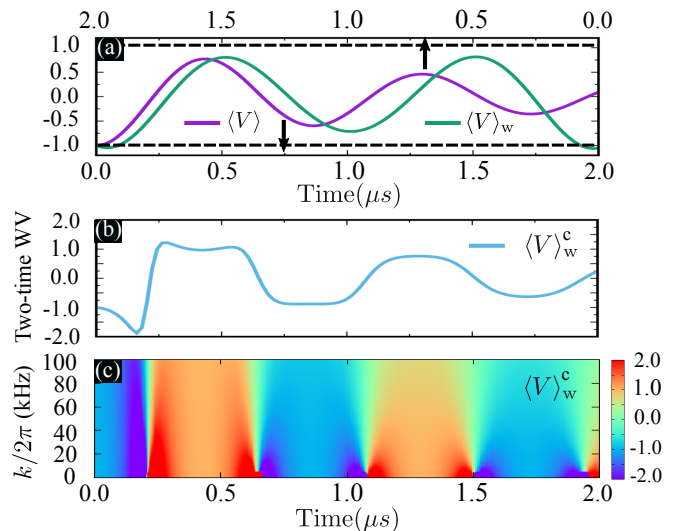


FIG. 4. (Color online) (a) The average values conditioned on the past (only) or the future (only) of the voltage signals (dark-violet curve.) The bottom axis corresponds the average of the voltage signal conditioned on the past density matrix prepared in the ground state. The state propagates forward in time under the master equation Eq. (20). The top axis is the average of the voltage signal conditioned on the future density matrix prepared in the ground state. The state propagates backward in time by the master equation Eq. (21). The vine-green curve is the conventional weak value of the voltage signal corresponded to the quantum state prepared and post-selected on the ground state. It is obtained from the enlarged quantum state  $\varrho_t$  as in Eq. (18). (b) The two-time weak value of the voltage signal at  $k/2\pi = 95$  kHz. (c) The two-time weak value of the voltage signal for a wide range of  $k$ , which is obtained from Eq. (19).

photon number tend to keep steady. In addition, the fluorescence signal in Fig. 3(c) shows a long decay between the two jumping durations. These effects can be seen clearly from the result in Fig. 3(d) extracted from the above Fig. 3(a-c) at the frequency  $\Omega/2\pi = 1.16$  MHz. We also note that these results are obtained from Eq. (12) by using the enlarged quantum state  $\varrho_t$ . One of the advances of using this enlarged quantum state is that we can obtain dynamically the measured value at any time  $0 \leq t \leq T$  that no need to wait until the final time  $T$ . We found that the two-time correlation weak values also exhibit the amplification effect as can be seen from Fig. 3, where the measured signals exceed outside the normal range  $[-1,1]$ . The results in Fig. 3(d) can apply to signal processing techniques. For example, one can clearly distinguish between the two levels of the atom population signal (e.g., “excited level” or “ground level”) because the signal keeps steady and therefore, its two-level can be triggered by setting a suitable threshold. Other kinds of signals, such as the photon number, the fluorescence signal, also can be explicitly detected.

As a second example, we apply our proposal to the case of weak continuously monitor a superconducting qubit

as described in Refs. [2, 3]. The corresponding master equations are given by [2, 3]

$$\frac{d\rho_t}{dt} = -\frac{i\Omega}{2}[\sigma_y, \rho_t] + k(\sigma_z \rho_t \sigma_z - \rho_t), \quad (20)$$

$$\frac{dE_t}{dt} = -\frac{i\Omega}{2}[\sigma_y, E_t] - k(\sigma_z E_t \sigma_z - E_t). \quad (21)$$

The enlarged master equation gives

$$\frac{d\varrho_t}{dt} = -\frac{i\Omega}{2}[\sigma_z \otimes \sigma_y, \varrho_t] + k[(\mathbf{I}_2 \otimes \sigma_z)\varrho_t(\mathbf{I}_2 \otimes \sigma_z) - \varrho_t]. \quad (22)$$

Let us focus on the voltage signal in this case. We use the same  $\Omega$  and  $k$  as above, i.e.,  $\Omega/2\pi = 1.16$  MHz and  $k/2\pi = 95$  kHz. In Fig. 4(a), the dark-violet curve displays the voltage signal conditioned on a single preselected density matrix  $\rho_0 = |g\rangle\langle g|$  or a single postselected density matrix  $E_T = |g\rangle\langle g|$ . These two values are the same in the time-reversal (we just see one curve because of the coincidence.) The result shows the damping effect as usual. Meanwhile, the vine-green curve in Fig. 4(a) exhibits the conventional weak value of the voltage signal, which is obtained from Eq. (18). Our study agrees with the previous study [2]. Figure 4(b) shows the jumping behavior of the two-time correlation weak value of the voltage signal for a fixed frequency at  $k/2\pi = 95$  kHz. Notable, the jump duration  $\Delta j$  increases in time at each fixed frequency. The effect even greater for a large range of  $k$  as shown in Fig. 4(c). The signal amplification effect is again observed as in the previous example.

## V. IMPLEMENTATION

In this section, we show that the  $\mathcal{ES}$  can be implemented in some physical platforms. Assume that the  $\mathcal{ES}$  is initially prepared in  $\varrho_0$  at time  $t = 0$  and its evolution is provided by the von Neumann equation as  $\varrho_t = \mathbf{U}_t \varrho_0 \mathbf{U}_t^\dagger$ , where  $\mathbf{U}_t = \exp[-\frac{i}{\hbar} \mathcal{H}t]$  and  $\mathcal{H} \equiv \sigma_z \otimes \mathbf{H}$  are the enlarged evolution and the enlarged Hamiltonian, respectively. The enlarged evolution  $\mathbf{U}_t$  can be implemented by using entangling Mølmer-Sørensen gates  $\mathbf{U}_{\text{MS}}$  as described in Ref. [12]. For example, to implement an  $\mathcal{ES}$  that consists of one  $\mathcal{OS}$  qubit and one ancillary qubit, we can prepare the initial enlarged state  $\varrho_0$  in the bases of a four-level system [39] in such way that it contains the pre- and postselected quantum states  $\rho_0$  and  $E_T$ , respectively. The enlarged evolution is given by

$$\mathbf{U}_t = \exp\left[-\frac{i\Omega}{2}(\sigma_z \otimes \sigma_y)t\right]. \quad (23)$$

To implement  $\mathbf{U}_t$ , we need (i) apply the Mølmer-Sørensen gate onto both the system qubit and the ancillary qubit, (ii) apply a local single-qubit rotation onto the ancillary qubit, and (iii) apply the Mølmer-Sørensen again. Following Ref. [40], we can implement  $\mathbf{U}_t$  by

$$\mathbf{U}_t = \mathbf{U}_{\text{MS}}\left(-\frac{\pi}{2}, \frac{\pi}{2}\right) e^{i\frac{\Omega t}{2}\sigma_x} \mathbf{U}_{\text{MS}}^\dagger\left(-\frac{\pi}{2}, \frac{\pi}{2}\right). \quad (24)$$

For the second example described in Sec. IV, the ancillary qubit is kept out of the environment and freely evolves under the system Hamiltonian  $\mathbf{H} \equiv \sigma_z$ . We can implement the  $\mathcal{ES}$  in a pair of qubits [41], where one qubit is driven at resonance with the cavity while the other is kept out of the resonance. We then also apply a sequence of the entangling Mølmer-Sørensen gates as we have already described above. The  $\mathcal{ES}$  thus can be implemented in superconducting circuits and also other physical systems, such as ion-traps [14, 42–44], quantum photonics [20]. In superconducting circuits, for example, one qubit is coupled to a cavity and plays the role of the  $\mathcal{OS}$ , while the remain qubit can be viewed as the ancillary qubit out of the cavity. Similarly, in ion-traps, one trapped ion can be addressed as the  $\mathcal{OS}$  resonance at laser frequency, while another trapped ion is the ancillary qubit and does not interact with the laser. In all cases, the ancillary qubit can be verified by changing the two-level energy splitting, using a magnetic field crossing the qubit [45].

## VI. DISCUSSIONS AND CONCLUSIONS

We remind that our proposal about the enlarged system ( $\mathcal{ES}$ ) in the enlarged Hilbert space plays the role of a quantum simulator, which is a one-to-one mapping between an original quantum system (the simulated system,  $\mathcal{OS}$ ) to a given mathematical model (the simulator system,) which is more controllable for reproducing the dynamics of the quantum system [46, 47]. The primary task of quantum simulators is to solve the dynamical time-dependent Schrödinger equation by fundamental laws of nature and also can be demonstrated in many physical models [47]. Specifically, in our case, the simulator system is the  $\mathcal{ES}$  where it simulates the forward and backward evolutions of the  $\mathcal{OS}$ . As a consequence, by continuous probing of the  $\mathcal{ES}$ , we also can control and gain the information in the  $\mathcal{OS}$ .

In conclusion, we found that the measured signals of an  $\mathcal{OS}$  bounded by past and future conditions can be monitored continuously in an  $\mathcal{ES}$ . Specifically, the weak value in the  $\mathcal{ES}$  is two-time correlated, which we name as the two-time correlation weak value. We showed that the two-time correlation weak value can be obtained dynamically at a given time by tracking the trajectory of the enlarged state. We have applied our proposal to the concept of a superconducting qubit driven by a laser field at the resonance frequency and shown the quantum jump effect in the measured signals. We have also observed the amplification effect of the two-time correlation weak value as well as its application in the signal processing techniques. Our proposal thus provides significant benefits in scientific and technological applications. It also can motivate and guide further various exciting experiments.

## ACKNOWLEDGMENTS

We would like to thank Y. Kondo of Kindai University for useful discussions. This work was supported by JSPS KAKENHI Grant Number JP19K14620.

### Appendix A: Master equation for an enlarged density matrix

The forward-evolving state propagates forward in time from the initial state  $\rho_0$  by the master equation

$$\frac{d\rho_t}{dt} = -\frac{i}{\hbar}[\mathbf{H}, \rho_t] + \sum_n \frac{1}{2} \left[ 2\mathbf{C}_n \rho_t \mathbf{C}_n^\dagger - \{\mathbf{C}_n^\dagger \mathbf{C}_n, \rho_t\} \right], \quad (\text{A.1})$$

and the backward-evolving state propagates backward in time from the final state  $E_T$  by the master equation

$$\frac{dE_t}{dt} = -\frac{i}{\hbar}[\mathbf{H}, E_t] - \sum_n \frac{1}{2} \left[ 2\mathbf{C}_n^\dagger E_t \mathbf{C}_n - \{\mathbf{C}_n^\dagger \mathbf{C}_n, E_t\} \right]. \quad (\text{A.2})$$

Because of the time symmetry in the measurement interval  $t \in [0, T]$ , we introduce an alternative “time-forward version” of the backward master equation Eq. (A.2), which evolves forward in time as

$$\frac{dE_{T-t}}{dt} = \frac{i}{\hbar}[\mathbf{H}, E_{T-t}] + \sum_n \frac{1}{2} \left[ 2\mathbf{C}_n^\dagger E_{T-t} \mathbf{C}_n - \{\mathbf{C}_n^\dagger \mathbf{C}_n, E_{T-t}\} \right]. \quad (\text{A.3})$$

For  $t = 0$ , the initial state is prepared by  $E_T$ , which corresponds to the postselection state. In other words, the postselection state is prepared at the beginning, in a similar manner to the previous work [12]. The solution of this equation at time  $t$  corresponds to  $E_{T-t}$ , which is also the solution of Eq (A.2) at time  $T - t$ .

We next define the enlarged quantum state as

$$\varrho_t \equiv \begin{pmatrix} [\varrho_t]^{00} & [\varrho_t]^{01} \\ [\varrho_t]^{10} & [\varrho_t]^{11} \end{pmatrix} = \frac{1}{2} \begin{pmatrix} \rho_t & 0_d \\ 0_d & E_{T-t} \end{pmatrix}, \quad (\text{A.4})$$

where  $[\varrho_t]^{ij}$  are  $d \times d$  block matrices. The combination of two forward master equations (A.1) and (A.3) in the following way will give the enlarged master equation

$$\frac{d\varrho_t}{dt} = -\frac{i}{\hbar} \left[ \begin{pmatrix} \mathbf{H} & 0_d \\ 0_d & -\mathbf{H} \end{pmatrix}, \varrho_t \right] + \sum_n \frac{1}{2} \left[ 2 \begin{pmatrix} \mathbf{C}_n & 0_d \\ 0_d & \mathbf{C}_n^\dagger \end{pmatrix} \varrho_t \begin{pmatrix} \mathbf{C}_n^\dagger & 0_d \\ 0_d & \mathbf{C}_n \end{pmatrix} - \left\{ \begin{pmatrix} \mathbf{C}_n^\dagger & 0_d \\ 0_d & \mathbf{C}_n^\dagger \end{pmatrix} \begin{pmatrix} \mathbf{C}_n & 0_d \\ 0_d & \mathbf{C}_n \end{pmatrix}, \varrho_t \right\} \right]. \quad (\text{A.5})$$

We set the enlarged operators  $\mathcal{H} \equiv \sigma_z \otimes \mathbf{H}$ ,  $\mathcal{C} \equiv |0\rangle\langle 0| \otimes \mathbf{C} + |1\rangle\langle 1| \otimes \mathbf{C}^\dagger$ , and  $\bar{\mathcal{C}} \equiv \mathbf{I}_2 \otimes \mathbf{C}$ , the enlarged master equation will give Eq. (6) in the main text.

For qubits case, we plot in Fig. 5 the quantum trajectories of the forward-evolving (left), the backward-evolving (right) and the enlarged (middle) quantum states in the  $x - z$  planes of the Bloch spheres against time. We consider here the resonance fluorescence case as in the main text with the pre and postselected states are given in the ground state. The red arrows indicate the direction of time evolution starting from  $t = 0$ . To illustrate the enlarged state, we divide it into block matrices  $[\varrho_t]^{ij}$  as shown in the figure. More precisely, we have  $[\varrho_t]^{00} = \rho_t/2$ ,  $[\varrho_t]^{01} = [\varrho_t]^{10} = 0_d$  ( $d = 2$  for the qubit case.) Specifically,  $[\varrho_t]^{11} = E_{T-t}/2$ , which is the time-reversal of  $E_t/2$  in the interval  $[0, T]$ .

### Appendix B: Analytical solution for the voltage signal in the enlarged system

Let us first decode the forward- and the backward-evolving states as follows

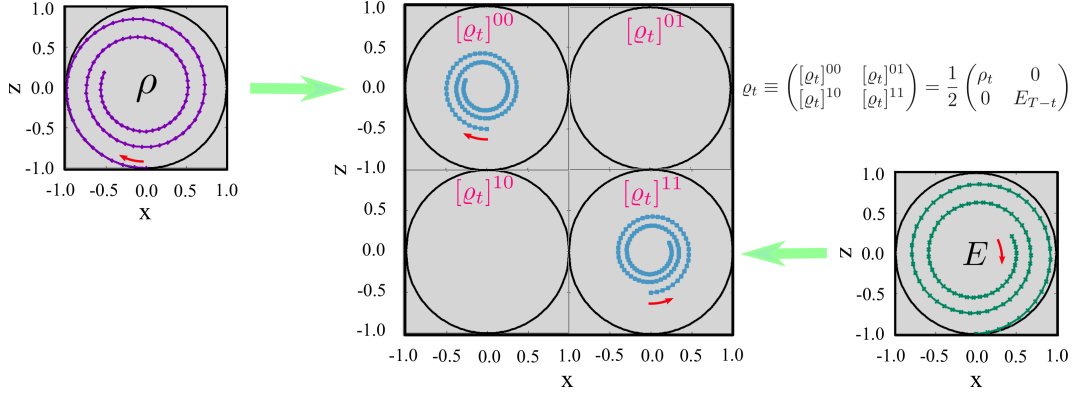


FIG. 5. (Color online) The quantum trajectories of the forward-evolving (left), the backward-evolving (right) and the enlarged (middle) quantum states in the  $x - z$  planes of the Bloch spheres against time. The red arrows indicate the direction of time evolution starting from  $t = 0$ .

$$\begin{aligned}
 \rho_t &= 2\mathcal{M}\varrho_t\mathcal{N} \\
 &= 2 \begin{pmatrix} 1 & 0 & 1 & 0 \\ 0 & 1 & 0 & 1 \end{pmatrix} \begin{pmatrix} \varrho_t^{00} & \varrho_t^{01} & \varrho_t^{02} & \varrho_t^{03} \\ \varrho_t^{10} & \varrho_t^{11} & \varrho_t^{12} & \varrho_t^{13} \\ \varrho_t^{20} & \varrho_t^{21} & \varrho_t^{22} & \varrho_t^{23} \\ \varrho_t^{30} & \varrho_t^{31} & \varrho_t^{32} & \varrho_t^{33} \end{pmatrix} \begin{pmatrix} 1 & 0 \\ 0 & 1 \\ 0 & 0 \\ 0 & 0 \end{pmatrix} \\
 &= 2 \begin{pmatrix} \varrho_t^{00} & \varrho_t^{01} \\ \varrho_t^{10} & \varrho_t^{11} \end{pmatrix}, \tag{B.1}
 \end{aligned}$$

where we have used the block matrices  $[\varrho_t]^{01} = [\varrho_t]^{10} = 0_d$ . Similarly, we also have

$$E_t = 2\mathcal{M}\varrho_{T-t}(\sigma_x \otimes \mathbf{I}_n)\mathcal{N} = 2 \begin{pmatrix} \varrho_{T-t}^{22} & \varrho_{T-t}^{23} \\ \varrho_{T-t}^{32} & \varrho_{T-t}^{33} \end{pmatrix}. \tag{B.2}$$

We now insert these two equations into the probability of the outcome of  $V_t$  of the continues measurement, which is defined by [48]

$$\begin{aligned}
 P(V) &= \frac{\text{Tr}(\Omega_V \rho_t \Omega_V^\dagger E_t)}{\sum_V \text{Tr}(\Omega_V \rho_t \Omega_V^\dagger E_t)} \\
 &\propto \varrho_t^{00} \varrho_{T-t}^{22} e^{-(V-1)^2/2a^2} + \varrho_t^{11} \varrho_{T-t}^{33} e^{-(V+1)^2/2a^2} + (\varrho_t^{10} \varrho_{T-t}^{23} + \varrho_t^{01} \varrho_{T-t}^{32}) e^{-(V^2+1)/2a^2}. \tag{B.3}
 \end{aligned}$$

Taking the integral over the outcome  $V$ , i.e.,  $\int P(V)VdV$ , the conventional weak value of the voltage signal is given by

$$\langle V \rangle_w = \frac{\varrho_t^{00} \varrho_{T-t}^{22} - \varrho_t^{11} \varrho_{T-t}^{33}}{\varrho_t^{00} \varrho_{T-t}^{22} + \varrho_t^{11} \varrho_{T-t}^{33} + \varrho_t^{10} \varrho_{T-t}^{23} + \varrho_t^{01} \varrho_{T-t}^{32}}. \tag{B.4}$$

This conventional weak value can be measured continuously, however, the forward-evolving and backward-evolving states are obtained separately as experimentally performed in Ref. [2, 3]. Even in our proposal of enlarged Hilbert space in this work, the conventional weak value only is acquired whenever the trajectories at time  $t$  and  $T - t$  are given. Nevertheless, for the two-time correlation weak value, the voltage signal gives

$$\langle V \rangle_w^c = \frac{\varrho_t^{00} \varrho_t^{22} - \varrho_t^{11} \varrho_t^{33}}{\varrho_t^{00} \varrho_t^{22} + \varrho_t^{11} \varrho_t^{33} + \varrho_t^{10} \varrho_t^{23} + \varrho_t^{01} \varrho_t^{32}}. \tag{B.5}$$

In this form, the two-time correlation weak value can be obtained dynamically by tomography the enlarged quantum state  $\varrho_t$  at time  $t$ , which is an advantage of our proposal for the “two-timer.”

- 
- [1] P. Campagne-Ibarcq, L. Bretheau, E. Flurin, A. Auffeves, F. Mallet, and B. Huard, *Phys. Rev. Lett.* **112**, 180402 (2014).
- [2] N. Foroozani, M. Naghiloo, D. Tan, K. Mølmer, and K. W. Murch, *Phys. Rev. Lett.* **116**, 110401 (2016).
- [3] D. Tan, S. J. Weber, I. Siddiqi, K. Mølmer, and K. W. Murch, *Phys. Rev. Lett.* **114**, 090403 (2015).
- [4] J. Dressel, A. Chantasri, A. N. Jordan, and A. N. Korotkov, *Phys. Rev. Lett.* **119**, 220507 (2017).
- [5] Y. Aharonov, D. Z. Albert, and L. Vaidman, *Phys. Rev. Lett.* **60**, 1351 (1988).
- [6] Y. Aharonov, S. Popescu, and J. Tollaksen, *Phys. Today* **63**, 27 (2010).
- [7] S. Wu and Y. Li, *Phys. Rev. A* **83**, 052106 (2011).
- [8] K. Nakamura, A. Nishizawa, and M. K. Fujimoto, *Phys. Rev. A* **85**, 012113 (2012).
- [9] D. Tan, N. Foroozani, M. Naghiloo, A. H. Küllerich, K. Mølmer, and K. W. Murch, *Phys. Rev. A* **96**, 022104 (2017).
- [10] L. P. Garcia-Pintos and J. Dressel, *Phys. Rev. A* **96**, 062110 (2017).
- [11] K. W. Murch, S. J. Weber, C. Macklin, and I. Siddiqi, *Nature* **502**, 211 (2013).
- [12] L. B. Ho, and N. Imoto, *Phys. Rev. A* **97**, 012112 (2018).
- [13] A. Silberfarb, P. S. Jessen, and I. H. Deutsch, *Phys. Rev. Lett.* **95**, 030402 (2005).
- [14] J. Casanova, C. Sabin, J. Leon, I. L. Egusquiza, R. Gerritsma, C. F. Roos, J. J. Garcia-Ripoll, and E. Solano, *Phys. Rev. X* **1**, 021018 (2011).
- [15] C. Noh, B. M. Rodriguez-Lara, and D. G. Angelakis, *Phys. Rev. A* **87**, 040102(R) (2013).
- [16] B. M. Rodriguez-Lara, and H. M. Moya-Cessa, *Phys. Rev. A* **89**, 015803 (2014).
- [17] X. Zhang, Y. Shen, J. Zhang, J. Casanova, L. Lamata, E. Solano, M.H. Yung, J.N Zhang, and K. Kim, *Nat. Commu* **6**, 7917 (2015).
- [18] R. DiCandia, B. Mejia, H. Castillo, J. S. Pedernales, J. Casanova, and E. Solano, *Phys. Rev. Lett.* **111**, 240502 (2013).
- [19] J. S. Pedernales, R. DiCandia, P. Schindler, T. Monz, M. Hennrich, J. Casanova, and E. Solano, *Phys. Rev. A* **90**, 012327 (2014).
- [20] J. C. Loredó, M. P. Almeida, R. Di Candia, J.S. Pedernales, J. Casanova, E. Solano, and A. G. White, *Phys. Rev. Lett.* **116**, 070503 (2016).
- [21] M. C. Chen, D. Wu, Z. E. Su, X. D. Cai, X. L. Wang, T. Yang, L. Li, N. L. Liu, C. Y. Lu, and J. W. Pan, *Phys. Rev. Lett.* **116**, 070502 (2016).
- [22] U. Alvarez-Rodriguez, J. Casanova, L. Lamata, and E. Solano, *Phys. Rev. Lett.* **111**, 090503 (2013).
- [23] L. B. Ho, *Phys. Lett. A* **383**, 289 (2019).
- [24] H. M. Wiseman and G. J. Milburn, *Quantum Measurement and Control* (Cambridge University Press, New York, 2010).
- [25] K. Jacobs and D. A. Steck, *Contemp. Phys.* **47**, 279 (2006).
- [26] S. Gammelmark, B. Julsgaard, and K. Mølmer, *Phys. Rev. Lett.* **111**, 160401 (2013).
- [27] B. Reznik and Y. Aharonov, *Phys. Rev. A* **52** 2358, (1995).
- [28] Y. Shikano and A. Hosoya, *J. Phys. A: Math. Theor.* **43**, 025304 (2010).
- [29] O. Oreshkov and C. Giarmatzi, *New J. Phys.* **18**, 093020 (2016).
- [30] R. Silva, Y. Guryanova, A. J. Short, P. Skrzypczyk, N. Brunner, and S. Popescu, *New J. Phys.* **19**, 103022 (2017).
- [31] L. Vaidman, A. Ben-Israel, J. Dziewior, L. Knips, M. Weiß, J. Meinecke, C. Schwemmer, R. Ber, and H. Weinfurter, *Phys. Rev. A* **96**, 032114 (2017).
- [32] Y. Aharonov and A. Botero, *Phys. Rev. A* **72**, 052111 (2005).
- [33] Y. Aharonov, S. Popescu, J. Tollaksen, and L. Vaidman, *Phys. Rev. A* **79**, 052110 (2009).
- [34] J. Koch, T. M. Yu, J. Gambetta, A. A. Houck, D. I. Schuster, J. Majer, A. Blais, M. H. Devoret, S. M. Girvin, and R. J. Schoelkopf, *Phys. Rev. A* **76**, 042319 (2007).
- [35] H. Paik, D. I. Schuster, L. S. Bishop, G. Kirchmair, G. Catelani, A. P. Sears, B. R. Johnson, M. J. Reagor, L. Frunzio, L. I. Glazman, S. M. Girvin, M. H. Devoret, and R. J. Schoelkopf, *Phys. Rev. Lett.* **107**, 240501 (2011).
- [36] R. Vijay, C. Macklin, D. H. Slichter, S. J. Weber, K. W. Murch, R. Naik, A. N. Korotkov, and I. Siddiqi, *Nature* **490**, 77 (2012).
- [37] S. J. Weber, A. Chantasri, J. Dressel, A. N. Jordan, K. W. Murch, and I. Siddiqi, *Nature* **511**, 570 (2014).
- [38] M. Abe and M. Ban, *Quantum Stud.: Math. Found.* **2**, 23 (2015).
- [39] M. J. Peterer, S. J. Bader, X. Jin, F. Yan, A. Kamal, T. J. Gudmundsen, P. J. Leek, T. P. Orlando, W. D. Oliver, and S. Gustavsson, *Phys. Rev. Lett.* **114**, 010501 (2015).
- [40] J. Casanova, A. Mezzacapo, L. Lamata, and E. Solano, *Phys. Rev. Lett.* **108**, 190502 (2012).
- [41] J. Majer, J. M. Chow, J. M. Gambetta, Jens Koch, B. R. Johnson, J. A. Schreier, L. Frunzio, D. I. Schuster, A. A. Houck, A. Wallraff, A. Blais, M. H. Devoret, S. M. Girvin, and R. J. Schoelkopf, *Nature* **449**, 443 (2007).
- [42] D. Leibfried, R. Blatt, C. Monroe, and D. Wineland, *Rev. Mod. Phys.* **75**, 281 (2003).
- [43] R. Batt, and C.F. Roos, *Nat. Phys.* **8**, 277 (2012).
- [44] L. Lamata, A. Mezzacapo, J. Casanova, and E. Solano, *EPJ Quant. Techn.* **1**, 9 (2014).
- [45] G. S. Paraoanu, *J. Low. Temp. Phys.* **175**, 633 (2014).
- [46] R. P. Feynman, *Int. J. Theor. Phys.* **21**, 467 (1982).
- [47] I. M. Georgescu, S. Ashhab, and F. Nori, *Rev. Mod. Phys.* **86**, 153 (2014).
- [48] S. Gammelmark, B. Julsgaard, and K. Mølmer, *Phys. Rev. Lett.* **111**, 160401 (2003).